Bioorganic & Medicinal Chemistry 17 (2009) 6311–6317

Contents lists available at ScienceDirect

Bioorganic & Medicinal Chemistry

journal homepage: www.elsevier.com/locate/bmc

Artemether/hydroxypropyl-β-cyclodextrin host–guest system: Characterization, phase-solubility and inclusion mode

Bo Yang [a,b], Jun Lin [a,*], Yong Chen [b], Yu Liu [b,*]

[a] School of Chemistry, Key Laboratory of Medicinal Chemistry for Natural Resource (Ministry of Education), Yunnan University, Kunming 650091, PR China
[b] Department of Chemistry, State Key Laboratory of Elemento-Organic Chemistry, Nankai University, Tianjin 300071, PR China

ARTICLE INFO

Article history:
Received 15 May 2009
Revised 15 July 2009
Accepted 16 July 2009
Available online 28 July 2009

Keywords:
Artemether
Hydroxypropyl-β-cyclodextrin
Characterization
Phase-solubility
Inclusion mode

ABSTRACT

An inclusion complex of the antimalarial artemether (ATM) in hydroxypropyl-β-cyclodextrin (HPβCD) was prepared and characterized. The phase-solubility diagram for the drug showed an increase in water solubility and gave an apparent binding constant of 220 M^{-1}. According to ^{1}H NMR and 2D NMR spectroscopy (ROESY), the inclusion mode involves two CH_3 from the drug orientated in the HPβCD cavity. The complex was characterized by Powder X-ray diffraction and thermal analysis. In addition, the complex produces a 1.81-fold enhancement in apparent bioavailability compared to artemether.

1. Introduction

Malaria has a devastating effect throughout tropical regions. There are approximately 300–500 million clinical cases each year resulting in 1.5–2.7 million deaths. Nearly all fatal cases are caused by *Plasmodium falciparum*.[1] The problem is compounded by the spread of drug resistant strains of the parasite. As a result, traditional alkaloid drugs such as chloroquine and quinine are now largely ineffective.[2] The spread of parasite resistance has led the World Health Organization (WHO) to predict that without new antimalarial drug intervention, the number of cases of malaria will have doubled by the year 2010.[3] Artemisinin (Qinghaosu) is a sesquiterpene 1,2,4-trioxane (sesquiterpene lactone endoperoxide) isolated from the Chinese medicinal herb qinghao (*Artemisia annua* L.). In 1979 it was shown to be an effective antimalarial against chloroquine-resistant strains of *P. falciparum*.[4] This compound and its derivatives, such as artemether (ATM), dihydroartemisinin, arteether, and artesunate, are effective against both chloroquine-resistant and chloroquine-sensitive strains of *P. falciparum*, as well as against cerebral malaria.[5,6] Most countries where malaria is endemic have adopted the WHO recommendation of artemisinin combination therapy (ACT) for fast and reliable malaria treatment.[7] However, artemisinin's poor solubility in both oil and water, and hydrolytic instability of the lactone function, have led scientists to prepare a series of semisynthetic first generation analogues, such as ATM (Chart 1).[8] Although ATM is a potent antimalarial, poor bioavailability and rapid clearance are observed with it and the other derivatives in both human and animal models.[9]

Cyclodextrins (CDs) are truncated-cone polysaccharides mainly composed of six to eight D-glucose monomers linked by α-1,4-glucose bonds. They have a hydrophobic central cavity and hydrophilic outer surface and can encapsulate model substrates to

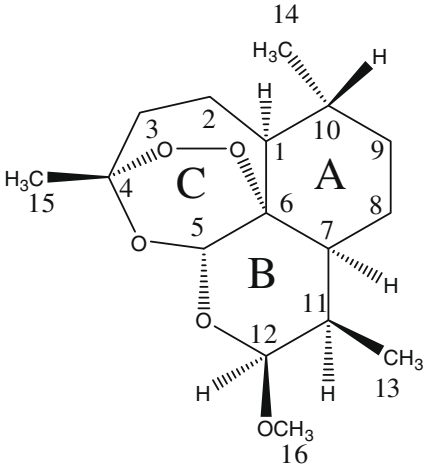

Chart 1. The structure of ATM.

* Corresponding authors. Tel./fax: +86 871 503 3215 (J.L.), tel./fax: +86 22 2350 3625 (Y.L.).
E-mail addresses: linjun@ynu.edu.cn (J. Lin), yuliu@nankai.edu.cn (Y. Liu).

0968-0896/$ - see front matter © 2009 Elsevier Ltd. All rights reserved.
doi:10.1016/j.bmc.2009.07.060

form host–guest complexes or supramolecular species. This usually enhances drug solubility in aqueous solution and affects the chemical characteristics of the encapsulated drug.[10–13] Hydroxypropyl-β-cyclodextrin (HPβCD, Chart 2) is a hydroxyalkylated βCD derivative that combines relatively high water solubility with low toxicity and satisfactory inclusion ability.[14,15] Several commercial formulations are composed of cyclodextrin inclusion complexes, illustrating the usefulness of this approach.[16–19]

The latest research indicates that HPβCD complexation with dihydroartemisinin increases dihydroartemisinin solubility and stability.[20] In this work we studied the formation of an inclusion complex of ATM with HPβCD. We utilized phase-solubility techniques, molecular modeling by ^{1}H NMR and 2D NMR spectroscopy (Rotating-frame Overhauser effect spectroscopy, ROESY) and characterized the complex by Powder X-ray diffraction and thermal analysis. We focused on the binding behaviors of hydroxypropyl-β-cyclodextrin with ATM and the solubilization effect of HPβCD toward ATM, as these may provide a useful approach to produce novel ATM formulations with high bioavailability.

2. Results and discussion

2.1. Phase-solubility

The phase-solubility diagram of the HPβCD/ATM system (Fig. 1) showed drug solubility increased linearly with increasing HPβCD concentration.

This diagram can be classified as A_L type according to the model proposed by Higuchi and Connors.[21] It can be related to the formation of a soluble inclusion complex. The apparent stability constant ($K_{1:1}$), was calculated from the linear fit of the curve according to the following equation:

$$K_{1:1} = \frac{Slope}{S_0(1 - Slope)}$$

where *Slope* is the value found in the linear regression and *So* is the aqueous solubility of the drug at pH 7 (*So* = 140 mg/l) in the absence of HPβCD, determined using HPLC by Hu.[22] This gave a $K_{1:1}$ of 220 ± 25 M^{-1} at 25 °C, suggesting a favorable interaction occurs as in general drug-CD association constants are reported in the range 50–2000 M^{-1}.[23]

2.2. Inclusion mode

In order to explore the possible inclusion mode of the HPβCD/ATM complex, we compared the ^{1}H NMR spectra of HPβCD in the absence and presence of ATM (Fig. 2). The ^{1}H resonances of HPβCD were assigned according to the reported method.[24,25] As illustrated in Figure 2, the majority of ATM chemical shifts were between δ 0.5 and 3 ppm and distinct from those of the HPβCD protons. After inclusion complexation with ATM, the H-3 proton of HPβCD shifted 0.010 ppm and the H-5 proton of HPβCD shifted 0.002 ppm (Table 1). Both H-3 and H-5 protons are located in the interior of the CD cavity, with H-3 protons near the wide side of cavity and H-5 protons near the narrow side. These results may indicate that ATM should be included in the HPβCD cavity from the wide side.

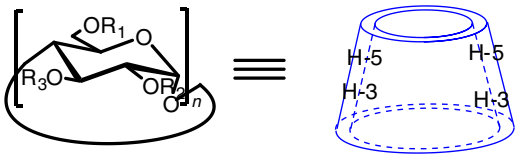

n=7 R_1=R_2=R_3=$CH_2CH(CH_3)OH$ or H HP-β-CD

Chart 2. The structure of HPβCD.

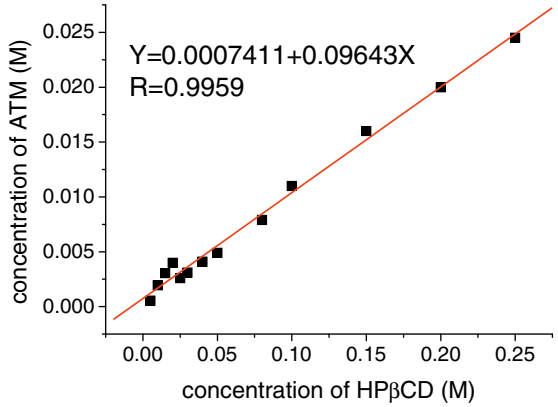

Figure 1. Phase-solubility diagram for the HPβCD/ATM host–guest system at 25 °C.

Two-dimensional (2D) NMR spectroscopy provides important information about the spatial proximity between host and guest atoms by observation of intermolecular dipolar cross-correlations. Two protons closely located in space can produce a nuclear Overhauser effect (NOE) cross-correlation in NOE spectroscopy (NOESY) or ROESY. The presence of NOE cross-peaks between protons from two species indicates spatial contacts within 0.4 nm.[26] To gain more conformational information, we obtained 2D ROESY of the inclusion complex of ATM with HPβCD (Fig. 3), including a partial contour plot (Fig. 3, inset). The ROESY spectrum of the HPβCD/ATM complex shows appreciable correlation of H-13 and H-14 protons of ATM with H-3 protons of HPβCD. No correlation is observed between H-5 and H-15 protons of ATM and H-5 or H-3 protons of the cyclodextrin. These results indicate that the CH_3 of the A and B rings of ATM are included in the HPβCD cavity. In combination with the 1:1 inclusion stoichiometry observed in the phase-solubility diagram, a possible inclusion mode for the HPβCD/ATM complex is proposed (Fig. 4).

2.3. X-ray diffraction of the inclusion complex

Powder XRD patterns allow examination of the medium and long range ordering of materials.[26] In contrast to the amorphous character of HPβCD (Fig. 5a), free ATM is a crystalline solid (Fig. 5b). The XRD pattern of the physical mixture confirmed the presence of both species as isolated solids, as the diffractogram showed both ATM peaks and the amorphous halo of HPβCD (Fig. 5c). The lyophilized inclusion complex has an amorphous structure (Fig. 5d), probably due to both the structure of HPβCD and the lyophilization process; this is evidence of the absence of ATM crystalline particles.

2.4. Thermal analysis of the inclusion complex

The thermal properties of the HPβCD/ATM complex were investigated by thermogravimetric analysis (TG) and differential scanning calorimetry (DSC). Analysis of the TG curves showed that ATM decomposes at ca. 170 °C (Fig. 6a) and HPβCD at ca. 360 °C (Fig. 6b). However, their inclusion complex had different thermal stability, with a decomposition temperature of ca. 365 °C (Fig. 6d). In contrast, the physical mixture of HPβCD and ATM apparently contains only the free species, as indicated by decomposition temperatures due to ATM at 170 °C and HPβCD at 360 °C (Fig. 6c). These results indicate that ATM's usual thermal properties were altered after inclusion complexation.

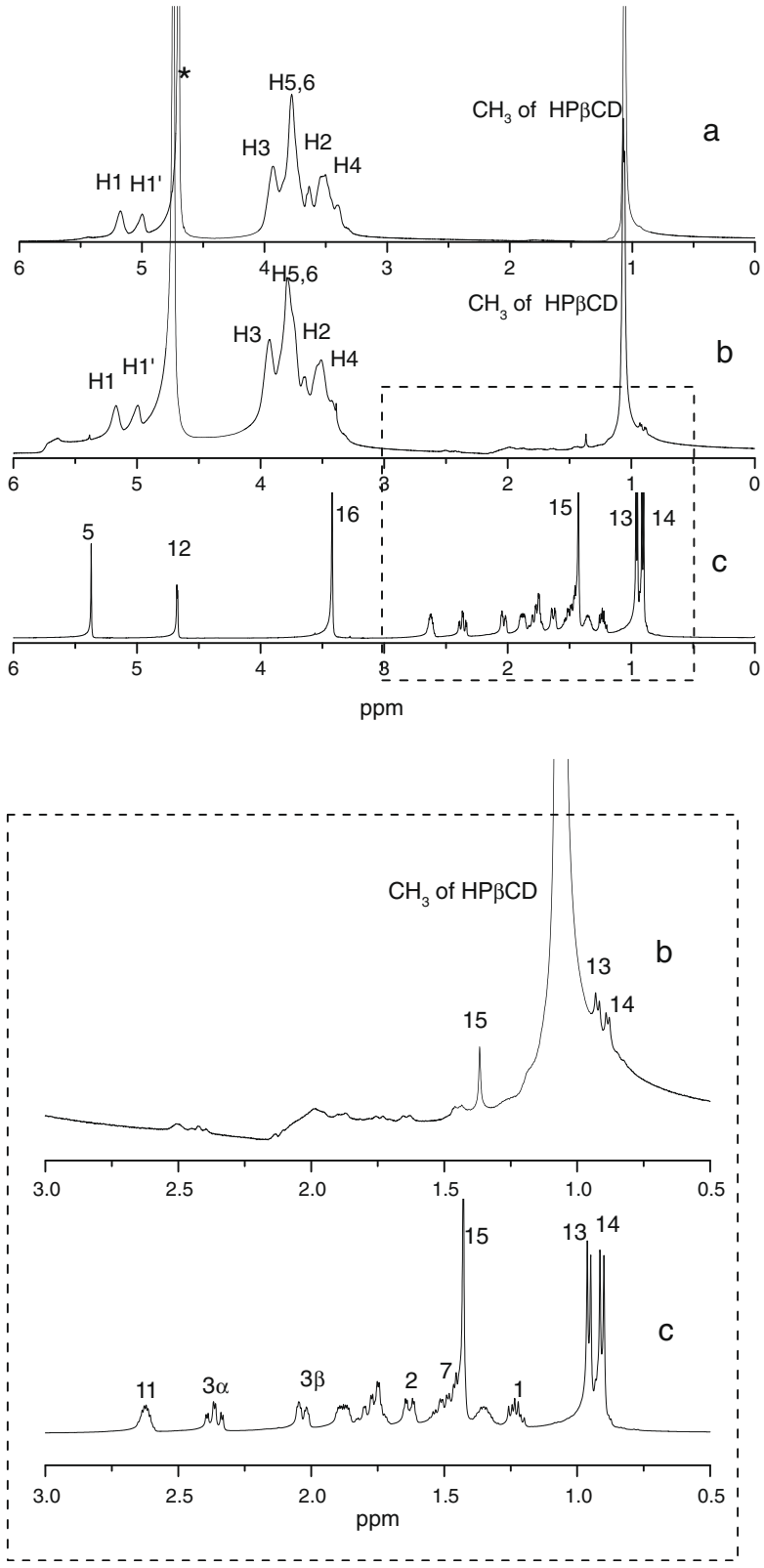

Figure 2. ^{1}H NMR spectra of HPβCD in the absence and presence of ATM in D_2O and ATM in $CDCl_3$ at 25 °C. (a) HPβCD, (b) HPβCD/ATM complex, (c) ATM (asterisk highlights the water peak, the window shows the enlarged NMR spectrum from approximately 0.5–3 ppm).

The differential scanning calorimetry (DSC) thermogram provides further information about the thermal properties of the HPβCD/ATM complex. The DSC curve of ATM displays an exothermic peak at 170 °C (Fig. 7a). In contrast, the DSC curve of pure HPβCD shows endothermic peaks at 80 and 360 °C (Fig. 7b), indicating HPβCD loses water at temperatures slightly above 80 °C and decomposes above 360 °C. The physical mixture of HPβCD and ATM apparently contains only the free species (Fig. 7c).

Table 1
The chemical shifts (δ) of HPβCD, HPβCD/ATM complex in D_2O and ATM in $CDCl_3$ at 25 °C

		δ (ppm)		
		ATM	HPβCD	HPβCD complex
H-1 of HPβCD	d	—	5.086	5.084
H-2 of HPβCD	dd	—	3.646	3.644
H-3 of HPβCD	dd	—	3.938	3.928
H-4 of HPβCD	dd	—	3.510	3.508
H-5 of HPβCD	m	—	3.778	3.780
H-6 of HPβCD	dd	—	3.778	3.780
CH_3 of HPβCD	dd	—	1.068	1.066
H-13 of ATM	d	0.951	—	0.924
H-14 of ATM	d	0.907	—	0.886
H-15 of ATM	s	1.428	—	1.367
H-5 of ATM	s	5.370	—	5.384

However, in the DSC curve of the HPβCD/ATM complex, the exothermic peak at about 170 °C corresponding to the free ATM disappears, while two new endothermic peaks appear at 80 and 365 °C (Fig. 7d). This suggests that the HPβCD/ATM complex is more stable than ATM. We propose that this result may be related to the complexation of HPβCD with ATM.

2.5. Bioavailability studies in the rats

The plasma concentration–time profiles of artemether are shown in Figure 8. The mean pharmacokinetic parameters derived from a non-compartmental analysis are presented in Table 2. Pharmacokinetic parameters obtained after parenteral administration of artemether suspension ($n = 6$) show a constant of C_{max} of 218.78 μg/ml, T_{max} of 89.32 min, and a AUC_{0-480} of 62038.65 μg min/ml. C_{max} of the complex (490.22 μg/ml) is higher than that of the suspension. This difference may be due to fast dissolution and absorption of the complex in the solution, a rapid and quantitative breakdown to yield high circulating concentrations once absorbed. On the other hand, T_{max} is significantly lower for the complex (29.52 min) in comparison to the artemether suspension. There is some difference between the AUC of complex (112137.89 μg min/ml) and the suspension. The apparent bioavailability of artemether following complex administration was found to be 181% compared to the artemether suspension. Thus, the results above indicated that complex had a much higher rate and extent of bioavailability compared to artmether suspension.

3. Conclusion

In summary, the complexation behavior, characterization and bioavailability of an inclusion complex of ATM with HPβCD were investigated. Results showed that HPβCD could enhance the water-solubility and bioavailability of ATM. Considering the lack of ATM applications, the complex could prove useful in the design of novel medicinal ATM formulations.

4. Experimental

4.1. Materials

ATM (FW = 298, PC >99%) was obtained from Kunming Pharmaceutical Corporation (Yunnan Province, P R China). Hydroxypropyl-

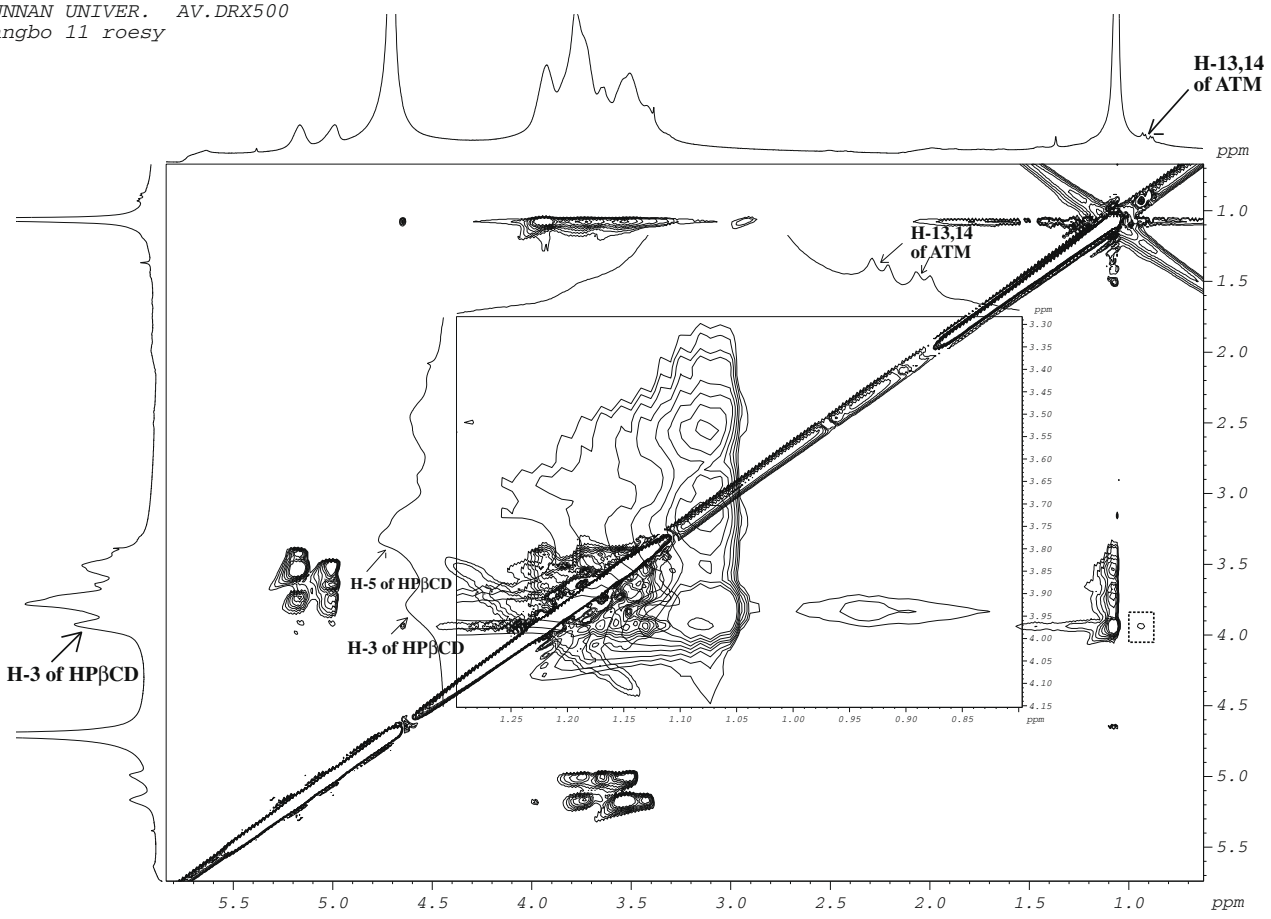

Figure 3. ROESY spectrum of the HPβCD/ATM complex in a D_2O.

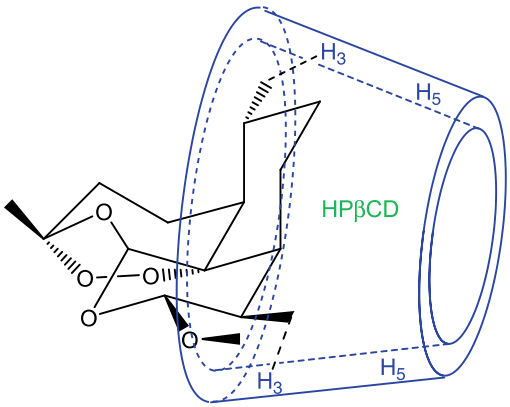

Figure 4. Possible inclusion mode of the HPβCD/ATM complex.

β-cyclodextrin (average FW = 1380) was purchased from Sigma–Aldrich Chemical Corporation (Shanghai, P R China) and used as received. Other reagents and chemicals were of analytical reagent grade. All experiments were carried out using ultrapure water.

4.2. HPLC assay

An Agilent 1100 HPLC system was used to determine the amount of ATM. The Agilent HPLC system was equipped with G1311A pump and controller, G1315B UV absorption detector, and G1313A autosampler. A Lichrospher C_{18} HPLC column (Hanbon, 5 μm, 150 mm × 4.6 mm, CHA) was used for separation and the mobile phase was water–acetonitrile (40:60, v/v). The injection volume was 20 μl and the effluent with a flow rate of 1.0 ml/min was monitored at an absorption wavelength of 210 nm.

4.3. Preparation of inclusion complexes

The inclusion complex was prepared by the suspension method.[27] This involved mixing of ATM and HPβCD in a 1:1 molar

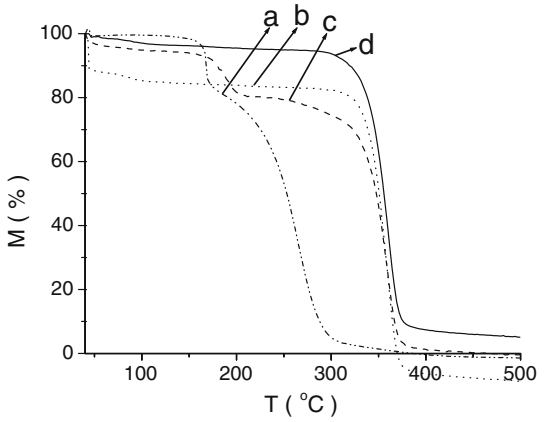

Figure 6. TG curves for: (a) ATM, (b) HPβCD, (c) HPβCD/ATM 1:1(mol proportion) physical mixture, and (d) HPβCD/ATM inclusion complex.

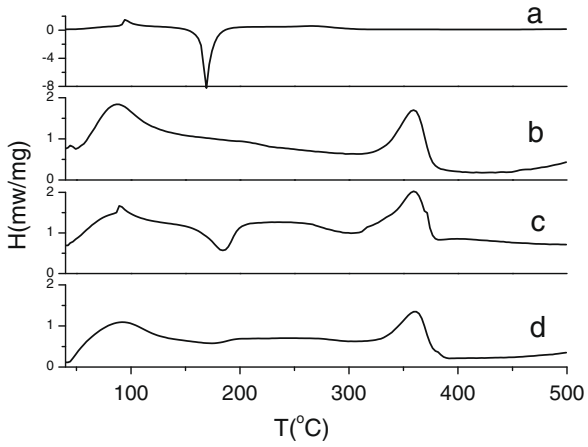

Figure 7. DSC curves for: (a) ATM, (b) HPβCD, (c) HPβCD/ATM1:1(mol proportion) physical mixture, and (d) HPβCD/ATM inclusion complex.

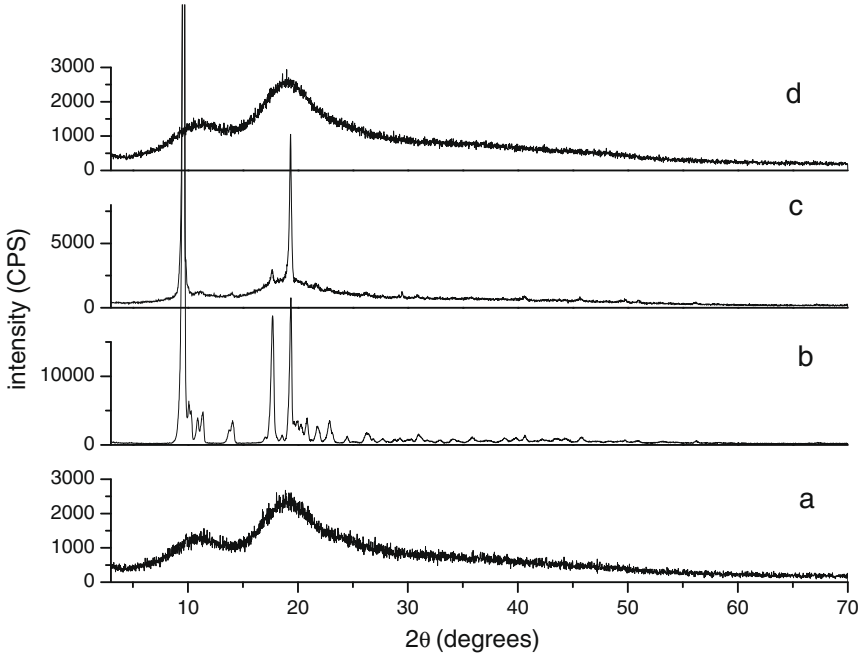

Figure 5. Powder X-ray diffractograms (Cu-κα) for: (a) HPβCD, (b) ATM, (c) HPβCD/ATM 1:1 (mol proportion) physical mixture, (d) HPβCD/ATM inclusion complex collected by lyophilization.

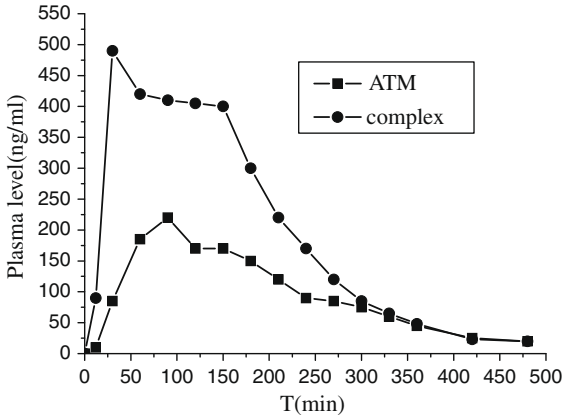

Figure 8. Artemether plasma concentration after administration of suspension (■) ($n = 6$), and artemether/HPβ-CD complex (●) ($n = 6$).

Table 2
Pharmacokinetic parameters and bioavailability of oral formulations

	C_{max} (ng/ml)	T_{max} (min)	AUC_{0-480}[a] (ng min/ml)	F_{app} (%)
Artemether (suspension)	218.78 ± 25.21	89.32 ± 15.66	62038.65 ± 2045.77	100
Artemether (complex)	490.22 ± 150.56	29.52 ± 5.44	112137.89 ± 4326.45	181

Results are mean ± S.D. of six determinations.
[a] AUC is for artemether.

proportion with stirring at room temperature for 48 h protected from light to prevent degradation. The solid residue was then separated by centrifugation at 15,000 rpm for 15 min and the upper liquid layer was filtered over a 0.45 μm Millipore membrane. The solution was then dried by lyophilization and the resulting solid inclusion complex collected.

A physical mixture, to test for possible inclusion, was prepared by grinding together a 1:1 molar mixture of HPβCD and ATM for 5 min with a small amount of water (the minimum amount to form a slurry) in an agate mortar.

4.4. Phase-solubility diagram

The phase-solubility diagram was studied according to the method proposed by Higuchi and Connors.[21] A series of HPβCD solutions were prepared with increasing concentrations: 0.01–0.25 M. A constant mass of ATM, in fivefold molar excess relative to the highest concentration HPβCD solution, was added to each solution and the suspensions stirred for 48 h in the dark. Following this, all suspensions were centrifuged and the supernatants were filtered over 0.45 μm Millipore membranes and analyzed by HPLC. This experiment was repeated three times.

4.5. Characterization of the complexes

^{1}H NMR spectra for HPβCD and ATM were obtained on a Bruker Avance DRX500 spectrometer at 298 K in D_2O and $CDCl_3$, respectively. ROESY experiments were run on a Bruker Avance DRX500 instrument. Samples were equilibrated for at least 24 hrs before measurement. All 2D NMR experiments were carried out in D_2O.

Powder X-ray diffraction (XRD) was measured in a D/max-3B diffractometer using Cu-κα ($k = 1{,}5460$ A°) with 30 mA, 40 kV, and a scanning rate of 5°/min. Powder samples were mounted on a sample holder and scanned with a step size of $2\theta = 0.02°$ between $2\theta = 3°$ and 70°.

Thermal analyses (TG and DSC) were recorded using a NETZSCH STA449F_3 instrument, with a 10 °C/min heating rate from room temperature to 500 °C and under N_2 flow (100 ml/min).

4.6. Bioavailability studies in the rats

Bioavailability studies in the rats were performed according to the reported method.[28]

Formulation preparation: artemether (60 mg) were suspended in 10 ml of an aqueous solution containing 0.5% of sodium methylcellulose; Oral solution was prepared by dissolving 2460 mg of artemether/hydroxypropyl-β-cyclodextrin complex in 10 ml of ddwater to make a concentration 6 mg/ml of artemether.

Rat experiment: Male Sprague–Dawley rats (weight range 280–300 g), after fasting overnight, were randomly treatmented the oral solution of artemether complex and artemether suspension ($n = 6$). The dosages were all 10.8 mg/day kg. Before blood sampling, the animals were anesthetized with diethyl ether. Blood samples of 0.4 ml were taken from the ophthalmic venus plexus and put into heparinized tubes at 12, 30, 60, 90, 120, 150, 180, 210, 240, 270, 300, 330, 360, 4200 and 4800 min after administration. The blood was immediately centrifuged at 4000 rpm for 10 min and 200 μl of plasma was quickly removed and stored at −20 °C until HPLC analyses.

Treatment of plasma samples: A 200 μl portion of plasma was added 50 μl 1% phosphoric acid solution and was vortexed for 3 min and kept for 5 min. Methanol (0.4 ml) was added and the mixture was vortexed for 3 min, then was centrifuged at 12,000 rpm for 10 min. The organic phase was transferred into new tubes and the contents evaporated to dryness under a stream of air at approximately 40 °C. The dried extracts were reconstituted with 150 μl of mobile phase solution, vortexed at high speed for 3 min, and centrifuged again at 12,000 rpm for 10 min. The entire volume of the reconstituted material (150 μl) was transferred to autosampler vials and 50 μl (sample volume) was injected onto the HPLC.

Pharmacokinetics and statistical analysis: The plasma concentration–time data of artemether were fitted by 3P87 Pharmacokinetics Program (The Section of Mathematical Pharmacology of Chinese Mathematical Pharmacological Society) and the pharmacokinetic parameters were calculated. The area under the concentration–time curve (AUC_{0-t}) was determined with trapezium method. C_{max} and T_{max} were determined through the observation of individual animal concentration versus time curses. The apparent bioavailability (F_{app}) of the artemether following administration of the complex was calculated by dividing the artemether AUC following complex dosing by that from suspension dosing. Statistical significance was indicated with $P < 0.01$.

Acknowledgments

Support for this work from the Opening Foundation of State Key Laboratory of Elemento-Organic Chemistry of Nankai University (0704 and 0815) and NSFC 30860342 are gratefully acknowledged, and we thank Zhao-Xiang Yang at Kunming Pharmaceutical Corporation, for his help on the bioavailability studies in the rats.

References and notes

1. Jomaa, H.; Wiesner, J.; Sanderbrand, S.; Altincicek, B.; Weidemeyer, C.; Hintz, M.; Tübachova, I.; Eberl, M.; Zeider, J.; Liechtenthaler, H. K.; Soldati, D.; Beck, E. *Science* **1999**, *285*, 1573.
2. O'Neill, P. M.; Pugh, M.; Stachulski, A. V.; Ward, S. A.; Davies, J.; Park, B. K. *J. Chem. Soc. Perkin Trans. 1* **2001**, 2682.
3. Foley, M.; Tilley, L. *Int. J. Parasitol.* **1997**, *27*, 213.
4. Klayman, D. *Science* **1985**, *228*, 1049.

5. WHO. In *The use of artemisinin and its derivatives as anti-malarial drugs. Report of a Joint CTD/DMP/TDR Informal Consultation*, World Health Organization: Geneva, 1998..
6. Bailint, G. A. *Pharma. Therap.* **2001**, *90*, 261.
7. WHO. In *Guidelines for the treatment of Malaria*, World Health Organization: Switzerland, 2006.
8. Baker, J. K.; Yarber, R. H.; Hufford, C. D.; ILee, S.; Elsohly, H. N.; McChesney, J. D. *Biomed. Environ. Mass Spectrom.* **1988**, *18*, 337.
9. Maggs, J. L.; Bishop, L. P. D.; Edwards, G.; O'Neill, P. M.; Ward, S. A.; Winstanley, P. A.; Park, B. K. *Drug Metab. Dispos.* **2000**, *28*, 209.
10. Szejtli, J. In *Cyclodextrin Technology*; Kluwer Academic: Dordrecht, 1988.
11. Uekama, K.; Hirayama, F.; Irie, T. *Chem. Rev.* **1998**, *98*, 2045.
12. Loftsson, T.; Järvinen, T. *Adv. Drug Delivery Rev.* **1999**, *36*, 59.
13. Loftsson, T.; Brewster, M. E. *J. Pharm. Sci.* **1996**, *85*, 1017.
14. Gould, S.; Scott, R. C. *Food Chem. Toxicol.* **2005**, *43*, 1451.
15. Castronuovo, G.; Niccoli, M. *Bioorg. Med. Chem.* **2006**, *14*, 3883.
16. Brewster, M. E.; Loftsson, T. *Pharmazie* **2002**, *57*, 94.
17. Duchene, D.; Wouessidjewe, D.; Poncel, G. *J. Controlled Release* **1999**, *62*, 263.
18. Irie, T.; Uekama, K. *J. Pharm. Sci.* **1997**, *86*, 147.
19. Davis, M. E.; Brewster, M. E. *Nat. Rev. Drug Discovery* **2004**, *3*, 1023.
20. Ansari, M. T.; Iqbal, I.; Sunderland, V. B. *Arch. Pharm. Res.* **2009**, *32*, 155.
21. Higuchi, T.; Connors, K. A. *Adv. Anal. Chem. Instrum.* **1965**, *4*, 117.
22. Hu, H.-Y.; Zhang, Z.-R. *HECHENG HUAXUE* **1999**, *7*, 334.
23. Loftsson, T.; Hreinsdóttir, D.; Masson, M. *Int. J. Pharm.* **2005**, *302*, 18.
24. Liu, Y.; Chen, C.-S.; Chen, Y.; Lin, J. *Bioorg. Med. Chem.* **2005**, *13*, 4037.
25. de Araújo, M. V. G.; Vieira, E. K. B.; Lázaro, G. S.; Conegero, L. S.; Almeida, L. E.; Barreto, L. S.; da Costa, N. B.; Gimeneza, I. F. *Bioorg. Med. Chem.* **2008**, *16*, 5788.
26. Correia, I.; Bezzenine, N.; Ronzani, N.; Platzer, N.; Beloeil, J.-C.; Doan, B.-T. *J. Phys. Org. Chem.* **2002**, *15*, 647.
27. Araujo, M. V. G.; Vieira, E. K. B.; Lazaro, G. S.; Conegero, L. S.; Ferreira, O. P.; Almeida, L. E.; Barreto, L. S.; Costa, N. B., Jr.; Gimenez, I. F. *Bioorg. Med. Chem.* **2007**, *15*, 5752.
28. Cao, F.; Guo, J.-X.; Ping, Q.-N.; Liao, Z.-G. *Eur. J. Pharm. Sci.* **2006**, *29*, 385.